Conserved Phosphoprotein Interaction Motif Is Functionally Interchangeable between Ataxin-7 and Arrestins †

ARTICLE *in* BIOCHEMISTRY · JULY 2000

Impact Factor: 3.02 · DOI: 10.1021/bi992694y · Source: PubMed

3 AUTHORS:

Arcady Mushegian
Independent Researcher
134 PUBLICATIONS **6,489** CITATIONS
SEE PROFILE

Sergey A Vishnivetskiy
Vanderbilt University
52 PUBLICATIONS **2,247** CITATIONS
SEE PROFILE

Vsevolod V Gurevich
Vanderbilt University
195 PUBLICATIONS **11,968** CITATIONS
SEE PROFILE

Conserved Phosphoprotein Interaction Motif Is Functionally Interchangeable between Ataxin-7 and Arrestins†

Arcady R. Mushegian, Sergey A. Vishnivetskiy, and Vsevolod V. Gurevich*

Ralph and Muriel Roberts Laboratory for Vision Science, Sun Health Research Institute, 10515 West Santa Fe Drive, Sun City, Arizona 85351

Received November 23, 1999; Revised Manuscript Received March 8, 2000

ABSTRACT: Olivopontocerebellar atrophy with retinal degeneration is a hereditary neurodegenerative disorder that belongs to the subtype II of the autosomal dominant cerebellar ataxias and is characterized by early-onset cerebellar and macular degeneration preceded by diagnostically useful tritan colorblindness. The gene mutated in the disease (*SCA7*) has been mapped to chromosome 3p12-13.5, and positional cloning identified the cause of the disease as CAG repeat expansion in this gene. The *SCA7* gene product, ataxin-7, is an 897 amino acid protein with an expandable polyglutamine tract close to its N-terminus. No clues to ataxin-7 function have been obtained from sequence database searches. Here we report that ataxin-7 has a motif of ca. 50 amino acids, related to the phosphate-binding site of arrestins. To test the relevance of this sequence similarity, we introduced the putative ataxin-7 phosphate-binding site into visual arrestin and β-arrestin. Both chimeric arrestins retain receptor-binding affinity and show characteristic high selectivity for phosphorylated activated forms of rhodopsin and β-adrenergic receptor, respectively. Although the insertion of a Gly residue (absent in arrestins but present in the putative phosphate-binding site of ataxin-7) disrupts the function of visual arrestin−ataxin-7 chimera, it enhances the function of β-arrestin−ataxin-7 chimera. Taken together, our data suggest that the arrestin-like site in the ataxin-7 sequence is a functional phosphate-binding site. The presence of the phosphate-binding site in ataxin-7 suggests that this protein may be involved in phosphorylation-dependent binding to its protein partner(s) in the cell.

The gene mutated in olivopontocerebellar atrophy with retinal degeneration has been recently cloned, and the disorder-associated mutation was identified (OMIM Entry 164500, *1*). The function of the putative ataxin-7 protein encoded by this gene is not known. To understand the molecular mechanisms of this hereditary disorder and to devise approaches for its treatment, we performed a detailed analysis of ataxin-7 sequence. We have identified a short element in ataxin-7 homologous to the phosphate-binding site of arrestins and used chimeric proteins to test the functionality of this putative site.

EXPERIMENTAL PROCEDURES

Mutagenesis. Chimeric arrestins were made by PCR. Common mutagenizing reverse primer introducing ataxin-7 sequence (5′-ctg tac ctt ccg gat gac cgc tct ccg ctg ggt caa gct atg cgt ttt gtc ctc -3′) was used in conjunction with visual-specific (5′-cct gac tac ctg ccc tgt tcg gtg-3′) or β-arrestin-specific (5′-atc cct ccg aac ctg cca tgc tct g-3′) forward primers to generate 88 or 79 bp fragments, respectively. The fragments were digested with *Sal*I and *Bsp*EI and subcloned into *Sal*I/*Bsp*EI-digested pARR and pBARR (*4*) plasmids, yielding pAV and pAB chimeras, respectively. A codon for an extra Gly residue (GGT) preceding Arg175 visual arrestin and AV chimera (Arg169 in β-arrestin and AB chimera) was also introduced by PCR. The sequence of all constructs was confirmed by dideoxy sequencing.

Direct Binding Assay. In vitro transcription and translation as well as receptor purification and phosphorylation were performed as described (*4, 5*). Translation of all proteins used for the direct binding assay yielded a single radiolabeled band with the expected electrophoretic mobility (not shown). The stoichiometry of phosphorylation of rhodopsin and β-adrenergic receptor (β_2AR)[1] used was 1.8 and 3.3 mol of phosphate/mol, respectively. In vitro translated radiolabeled arrestins (50 fmol) were incubated in 50 mM Tris-HCl, pH 7.5, 0.5 mM $MgCl_2$, 1.5 mM dithiothreitol, 50 mM potassium acetate with 7.5 pmol of the various functional forms of rhodopsin or with 100 fmol/assay of P-β_2AR or β_2AR in a final volume of 50 μL for 5 min at 37 °C in room light (rhodopsin) or for 35 min at 30 °C in the presence of 0.1 mM β-agonist isoproterenol (β_2AR). The samples were then cooled on ice and loaded onto 2 mL Sepharose 2B columns equilibrated with 10 mM Tris-HCl, pH 7.4, 100 mM NaCl. Bound arrestin eluted with receptor-containing membranes in the void volume (between 0.5 and 1.1 mL). Nonspecific binding was subtracted. It was determined in the presence of 0.3 μg of liposomes and did not exceed 0.4 fmol/assay. We have previously established that nonspecific "binding"

† This work was supported in part by National Institutes of Health Grant EY 11500 (to V.V.G.).

* Corresponding author. Telephone: (623) 876-5462; Fax: (623) 876-6663; E-mail: vsevolod_gurevich@mail.sunhealth.org.

[1] Abbreviations: β_2AR, β_2-adrenergic receptor; P-β_2AR, phosphorylated β_2AR; Rh*, light-activated rhodopsin; P-Rh*, phosphorylated Rh*; P-Rh, dark phosphorylated rhodopsin; Rh, dark rhodopsin; RMS, root-mean-square deviation.

10.1021/bi992694y CCC: $19.00
Published on Web 05/18/2000

```
consensus                          Dxxkxc G x U = U = x + x u c o x x u x x x x x + x h x x x x x r x U x x + + x x U x x
Ataxin-7                2370153 341 DPDIHCGVIDLDTKKPCTRSLTC---KTHSLTQRRAVQGRRKRFDV 508
Arrestin beta/bovine     162692 134 DTGKACG-VDYEVKAFCAENLEE---KIHKRNSVRLVI-RKVQYAP 243
Arrestin visual/bovine  4929981 137 DVGKSCG-VDFEIKAFATHSTDVEEDKIPKKSSVRLLI-RKVQHAP 187
Arrestin beta 2/human   4757780 135 DTGKACG-VDFEIRAFCAKSLEE---KSHKRNSVRLVI-RKVQFAP 233
Arrestin C/Human        3892697 131 DAGKPCG-IDFEVKSFCAENPEE---TVSKRDYVRLVV-RKVQFAP 216
ARRB_DROME               114211 150 DNGKPLG-VEYTIRAFVGDSEDD---RQHKRSMVSLVI-KKLQYAP 228
YGG6_YEAST              1723846 243 DFNKQCG-VELPEGGYCARSLTC---KSHSMGAKRAVSGRSKPYDV 322
CAA22473.1/Sch.pombe    4008552 197 DVEKQCG-VLLPNGQMCARSLTC---KTHSMSSKRAVPGRSQPYDV 105
Secondary - pdb 1CF1C                bbbbbbbbbbbbbbb        bbbbbbb~bbbbb
                                                              *     **
```

FIGURE 1: Conserved sequence motif in ataxin-7 and diverse arrestins. Multiple sequence alignment of ataxin-7, yeast homologues, and diverse arrestins was constructed using the MACAW program (*15*). Unique sequence identifiers in GenBank are shown after protein names. Numbers indicate distances to the ends of each protein. Conserved amino acids are shown in boldface type. Bulky hydrophobic residues (I, L, M, V, F, Y, and W) are shaded and shown as "U" in the consensus line; acidic residues (D or E) as "="; basic residues (K and R) as "+"; and small side chain residues (A, G, and S) as "O". Known elements of the three-dimensional structure in bovine arrestin are indicated (b, β-strand). The box shows the segments exchanged in AB, ABG, AV, and AVG chimeras. See the text for other designations.

observed in the presence of 0.3 μg of opsin-containing membranes and 0.3 μg of liposomes is virtually identical (*5*). This "binding" mostly represents a small percentage of arrestin (less than 1%) that aggregates during the assay and coelutes with receptor-containing membranes (*17*). The use of high molar excess of rhodopsin over arrestin in the direct binding assay is necessary for two reasons. Light-activated rhodopsin decays into inactive opsin within minutes, necessitating a short incubation time. On the other hand, the high molecular weight of arrestin makes its diffusion-limited "on-rate" relatively slow (e.g., arrestin binding to P-β_2AR reaches equilibrium in about 30 min). Incubation of arrestin for 5 min with a 75−150-fold excess of rhodopsin was found to be the best way to perform this unavoidably nonequilibrium binding assay (*5*, *17*).

RESULTS AND DISCUSSION

We partitioned the sequence of the 897 amino acid ataxin-7 into globular and nonglobular regions using the SEG program (*2*). More than 60% of the sequences fall into predicted nonglobular regions. The three longest globular regions were used to scan sequence databases with the PSI-BLAST program (*3*). A significant similarity (score, $s = 123$, probability of matching by chance, $p = 4 \times 10^{-7}$) was observed between a globular region in ataxin-7 corresponding to amino acids 338−393 and a putative protein in fission yeast (gi4008552). An alignment of these ataxin-7 and yeast sequences was converted into a profile, and the WiseTools program (*13*) was used to search protein databases for additional homologues. A significant similarity (score > 5000) was observed between these proteins and arrestins, a group of animal proteins that specifically bind to the activated phosphorylated forms of G protein-coupled receptors (*4*) and quench their signaling. Motif search with the ungapped subalignment of ataxin-7 and yeast homologues using the program MoST (*14*) with a restrictive cutoff ratio $r = 0.01$ also identified more than 25 arrestins (and no other sequences) before convergence. Further analysis (Figure 1) detected a motif of about 50 amino acids shared between ataxin-7, both yeast proteins, and arrestins.

Structure−function studies of chimeric, truncated, and mutant arrestins have identified elements that are directly involved in receptor binding (*4*, *5*). Interestingly, the region of similarity to ataxin-7 includes the entire phosphorylation-recognition site of arrestins (*4*−*11*). All three positively charged residues crucial for interaction with a phosphate on a phosphoreceptor are conserved in ataxin-7 (Figure 1, indicated by the asterisks). These include the arginine residue serving as a key phosphorylation-sensitive trigger in both β-arrestin and visual arrestin (*6*−*9*, *11*) (green-shaded column in Figure 1). In addition, a bulky hydrophobic residue that hinders arrestin interaction with unphosphorylated receptor (*7*) (underlined in Figure 1) and also the upstream region with an acidic residue that forms a salt bridge with Arg171 in visual arrestin (*10*, *11*) (double underline) are also conserved.

The key functional characteristic of arrestin proteins is their strict selectivity for phosphorylated activated forms of their cognate receptors (*4*, *5*, *9*, *11*). The binding to activated phosphoreceptor involves a substantial conformational rearrangement in arrestin molecule (*5*, *11*, *18*). The X-ray crystal structure of the basal state of bovine visual arrestin has been recently resolved, revealing all-β fold in the N-terminal domain (*10*, *11*), where the phosphate-binding site is located (*6*). The region of similarity to ataxin-7 and yeast proteins includes two β-strands (IX and X in ref *11*) located on the concave surface of the N-terminal domain. This domelike surface lined with positive charges is believed to be the docking site for the cytoplasmic tip of the rhodopsin molecule (*10*, *11*). Several of the positively charged residues localized on β-strand X (*11*) were shown to play a crucial role in the preferential binding of arrestin to phosphorylated receptors (*6*, *7*).

Arrestins' selectivity for phosphorylated forms of their cognate receptors is ensured by an ingenious mechanism. There is an unusual network of buried solvent-excluded positively and negatively charged residues ("polar core") in the fulcrum of the two-domain arrestin molecule (*11*). Charge reversal mutations of polar core residues relieve the arrestin requirement for receptor phosphorylation, yielding "constitutively active" phosphorylation-independent mutants (*6*−*9*, *11*). Various combinations of these charge-reversal mutations that restore the charge balance of the polar core also restore arrestin selectivity toward phosphoreceptors (*9*, *11*). We hypothesized that the receptor-attached phosphate is "guided" by the positive charges in the cavity of the N-domain toward the polar core, where it upsets the polar core's charge balance and allows arrestin to undergo a

conformational transition into its active receptor-binding state (*9, 11*). This mechanism explains how arrestins bind to heterogeneous species of phosphorylated receptors with different numbers of phosphate moieties attached to the receptor COOH-terminus (e.g., rhodopsin, β-adrenoreceptor) or the third intracellular loop (e.g., m2 muscarinic cholinergic receptor) (*4*−*6, 9, 11*).

Thus, a functional phosphate-binding site (homologous or heterologous) in the β-strand X in the arrestin sequence can be expected to draw a phosphate to the polar core with the resultant arrestin transition into its active state and high-affinity binding to phosphoreceptors. In this model, a relatively weak protein−phosphate interaction is translated into a strong, easily measurable arrestin−receptor interaction. Virtually any mutation in the arrestin phosphate-binding site has detectable functional consequences (*6*−*9*), allowing for unambiguous discrimination between functional and nonfunctional putative phosphate-binding elements. Screening the engineered arrestin-based chimeras for their binding selectivity for phosphoreceptors appears to be a sensitive test for the functionality of phosphate-binding elements. The major limitation of this approach is that the putative phosphate-binding element needs to be contiguous and relatively short, so that it fits into β-strand X and does not interfere with the proper folding and conformational flexibility of the arrestin molecule.

On the basis of sequence similarity, we hypothesized that an element of ataxin-7 (Figure 1) may be involved in phosphorylation-dependent interaction with a yet unidentified protein partner(s). To test the functionality of the putative phosphate-binding site in ataxin-7, we constructed ataxin−visual arrestin chimeric protein AV and ataxin−β-arrestin chimera AB, in which the ataxin-7 sequence THSLTQRRAV substitutes visual arrestin residues 164−173 (IPKKSSVRLL) or β-arrestin residues 158−167 (IHKRNSVRLV), respectively (Figures 1 and 3). The β-strand X in these two chimeras has the same length as in parental arrestin proteins. To test the role of an "inserted" (as compared to arrestins) glycine residue upstream of the two additional positive charges in the phosphate-binding site, we have also constructed AVG and ABG chimeras. These proteins are similar to AV and AB, respectively, but have a characteristic for an ataxin-7 additional Gly residue inserted before the Arg-Lys pair (Figure 1). To evaluate the effect of this Gly insertion (which lengthens β-strand X at a sensitive place) on arrestin folding and function, we have also constructed arrestin-(iG175) (AG) and β-arrestin(iG169) (BG) mutants. VG mutant and both AV and AVG chimeras were expressed in the in vitro translation system, and their binding to four functional forms of rhodopsin (dark phosphorylated; light-activated phosphorylated, P-Rh*; dark unphosphorylated; light-activated unphosphorylated) was compared to that of visual arrestin (Figure 2A).

Both VG mutant and AV chimera demonstrate high binding to P-Rh*, although it is somewhat lower than that of wild-type visual arrestin. Both mutant forms faithfully reproduce arrestin selectivity for this functional form of rhodopsin (Figure 2A). However, the binding of AVG chimera to rhodopsin is reduced dramatically. There are two conceivable reasons for this apparent lack of activity: the protein could be misfolded, or it may fail to assume its active high-affinity receptor-binding conformation upon encountering P-Rh*. Misfolded or denatured proteins typically express at a very low level in rabbit reticulocyte lysate, being rapidly degraded by endogenous proteases, and a large (>70%) fraction of the misfolded protein aggregates and ends up in the pellet after the high-speed centrifugation we routinely perform after translation (*17, 19*). However, the expression levels of VG, AV, and AVG (45−60 fmol/μL), as well as the percentage of these proteins that remain in the supernatant (75−85%), were similar to those of wild-type arrestin (50 fmol/μL and 80−90%, respectively). Apparently, low binding of AVG does not reflect a folding problem.

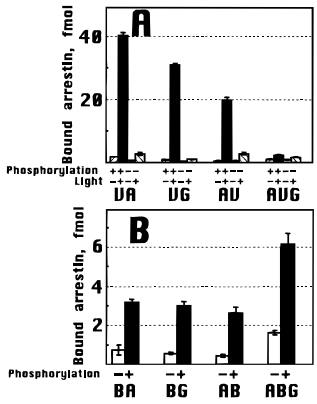

FIGURE 2: Binding characteristics of visual arrestin, β-arrestin, and chimeric arrestins with ataxin-7 sequence. In vitro translated radiolabeled arrestins (100 fmol) (specific activities 151−192 dpm/fmol) were incubated in a final volume of 50 μL for 5 min at 37 °C with 7.5 pmol of the indicated functional forms of rhodopsin (A), or for 35 min at 30 °C with P-β_2AR or β_2AR (100 fmol/assay) in the presence of 100 μM agonist isoproterenol (B). The samples were immediately cooled on ice and loaded onto 2 mL Sepharose 2B columns equilibrated with 10 mM Tris-HCl, pH 7.4, 100 mM NaCl. Bound arrestin eluted with receptor-containing membranes in the void volume (between 0.5 and 1.1 mL). Nonspecific binding determined in the presence of 0.3 μg of liposomes was subtracted. Each protein was translated twice, and 2 binding experiments (in duplicate) were performed with each batch. Means ± SD of 4 experiments are presented.

Similarly expressed BG mutant, AB, and ABG chimeras fully retain the binding characteristics of β-arrestin including its preference for phosphorylated receptor (in this case, the β2AR; Figure 2B). In sharp contrast to AVG, ABG chimera even demonstrates a substantially higher binding to P-β2AR* than parental wild-type protein. Notably, in the case of β-arrestin, neither the insertion of a glycine residue nor the introduction of ataxin-7 sequence appreciably reduces P-β2AR* binding.

We used the ProMod algorithm, which uses the coordinates of the backbone atoms for initial modeling but permits backbone flexibility at the refinement stage (*16*), and the three-dimensional structure of visual arrestin (*11*) to model the structural effects of sequence changes in the AV and AVG chimeras (Figure 3). In the AV chimera, the backbone of the ataxin-7-derived 10 amino acid peptide is predicted to adopt the conformation similar to that of the replaced fragment (RMS of the 40 backbone atoms, $r = 1.82$ Å). A bulky side chain of arginine R170 in the AB and AV chimeras replaces a shorter arrestin-specific side chain of valine V170. However, the side chain clash is avoided because of the "compensatory" change of leucine L172 (typical for arrestins) into alanine in ataxin-7 (Figure 3, middle panel). In the AVG chimera, a bulge comprising the

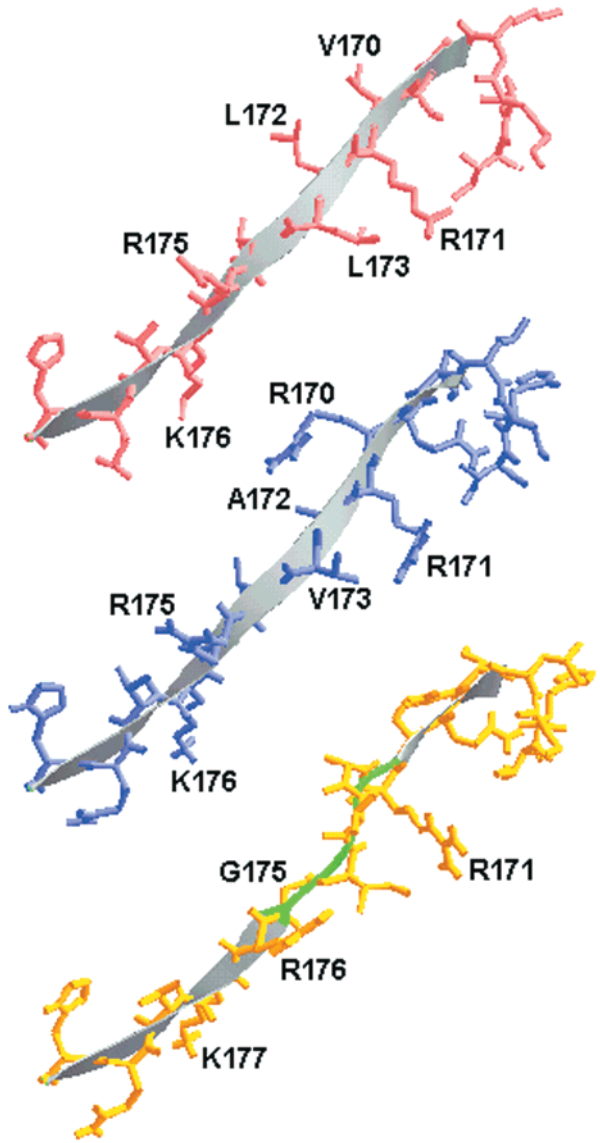

FIGURE 3: Native structure of bovine visual arrestin and structural model of the ataxin-7-specific peptide in the AV and AVG chimeras. Only β-strand X and the adjoining turns are shown. Top panel: native bovine visual arrestin (pdb ID 1CF1). Middle panel: AV chimera. Bottom panel: AVG chimera. The amino acids mentioned in the text are labeled according to their positions in the wild-type or mutant proteins. The bulge in the AVG chimera is shown as a green backbone. The model was built using the ProMod algorithm on the Swiss-Model server (*16*).

inserted glycine and three upstream residues is predicted (Figure 3, bottom panel). Two of these upstream residues are part of the ataxin-7-derived peptide, and the overall shape of that peptide is likely to be distorted (RMS of the 40 backbone atoms in the AVG model is 2.78 Å). The orientation of the side chains in downstream residues (including those of the functionally important Arg-Lys pair) is also changed (Figure 3, bottom panel). Similar although less dramatic distortion of the backbone and side chains was observed in a model of the VG mutant (not shown).

The replacement of 10 amino acids in visual arrestin affects mostly the structure and orientation of the side chains, whereas glycine insertion affects the orientation of the backbone and side chains. While these two modifications have only a mild effect on the interaction of visual arrestin with the receptor, their combination appears to have a cumulative effect. Interestingly, similar effects were not observed when the same modifications were made in β-arrestin. Preliminary crystallographic data suggest that the atom density in the N-terminal domain of β-arrestin is lower than in the case of visual arrestin (C. Schubert and V. V. Gurevich, unpublished observations). Less dense packing of β-arrestin may be the reason it accommodates "ataxin-7-like" changes easier than visual arrestin. Comparison of high-resolution crystal structures of both proteins is needed for a detailed mechanistic explanation.

To summarize, the binding characteristics of AV, AB, and ABG chimeras suggest that the homologous ataxin-7 sequence placed in the context of visual arrestin or β-arrestin functions as an efficient phosphate-binding site, supporting the idea that this sequence in ataxin-7 may be involved in binding to phosphorylated proteins. In ataxin-7 and in both yeast proteins, the arrestin-like motifs comprise the globular regions of 45−60 amino acids, flanked by longer nonglobular segments (not shown). Given that the nonglobular regions are believed to be elongated and poorly structured (*2*), the arrestin-related motifs are likely to be independently folding units. In contrast, the phosphorylation-recognition motif in arrestins is part of a larger all-β fold. In the course of evolution, this motif might have blended into arrestins by recombinational β-strand invasion (*12*).

The biochemical functions of ataxin-7 (as well as those of yeast proteins identified in our homology search) remain to be elucidated. We believe that our data suggest the existence of protein interaction partner(s) and narrow down the search to the phosphorylated proteins. The putative phosphate-binding site described here may be joining the collection of protein domains with phosphate-binding function, such as the 14-3-3 domain and the SH2 domain (http://coot.EMBL_Heidelberg.de/SMART). The functionality and relative portability of such a small conserved region also have implications for our understanding of protein folding and evolution.

ACKNOWLEDGMENT

We thank Dr. J. L. Benovic for purified β-adrenergic receptor kinase (GRK2), Dr. J. G. Krupnick for purified rhodopsin kinase (GRK1), and Dr. J. J. Onorato for purified β_2AR.

REFERENCES

1. David, G., Abbas, N., Stevanin, G., Durr, A., Yvert, G., Cancel, G., Weber, C., Imbert, G., Saudou, F., Antoniou, E., Drabkin, H., Gemmill, R., Giunti, P., Benomar, A., Wood, N., Ruberg, M., Agid, Y., Mandel, J. L., and Brice, A. (1997) *Nat. Genet. 17*, 65−70.
2. Wootton, J. C., and Federhen, S. (1996) *Methods Enzymol. 266*, 554−573.
3. Altschul, S. F., Madden, T. L., Schaffer, A. A., Zhang, J., Zhang, Z., Miller, W., and Lipman, D. J. (1997) *Nucleic Acids Res. 25*, 3389−3402.
4. Gurevich, V. V., Dion, S. B., Onorato, J. J., Ptasienski, J., Kim, C. M., Srterne-Marr, R., Hosey, M. M., and Benovich, J. L. (1995) *J. Biol. Chem. 270*, 720−731.
5. Gurevich, V. V., and Benovic, J. L. (1993) *J. Biol. Chem. 268*, 11628−11638.
6. Gurevich, V. V., and Benovic, J. L. (1995) *J. Biol. Chem. 270*, 6010−6016.
7. Gurevich, V. V., and Benovic, J. L. (1997) *Mol. Pharmacol. 51*, 161−169.

8. Kovoor, A., Celver, J., Abdryashitov, R. I., Chavkin, C., and Gurevich, V. V. (1999) *J. Biol. Chem. 274*, 6831−6834.
9. Vishnivetskiy, S. A., Paz, C. L., Schubert, C., Hirsch, J. A., Sigler, P. B., and Gurevich, V. V. (1999) *J. Biol. Chem. 274*, 11451−11454.
10. Granzin, J., Wilden, U., Choe, H. W., Labahn, J., Krafft, B., and Buldt, G. (1998) *Nature 391*, 918−921.
11. Hirsh, J. A., Scubert, C., Gurevich, V. V., and Sigler, P. B. (1999) *Cell 97*, 257−269.
12. Chothia, C., Hubbard, T., Brenner, S., Barns, H., and Murzin, A. (1997) *Annu. Rev. Biophys. Biomol. Struct. 26*, 597−627.
13. Birney, E., Thompson, J. D., and Gibson, T. J. (1996) *Nucleic Acids Res. 24*, 2730−2739.
14. Tatusov, R. L., Altschul, S. F., and Koonin, E. V. (1994) *Proc. Natl. Acad. Sci. U.S.A. 91*, 12091−12095.
15. Schuler, G. D., Altschul, S. F., and Lipman, D. J. (1991) *Proteins: Struct., Funct., Genet. 9*, 180−190.
16. Guex, N., and Peitsch, M. C. (1997) *Electrophoresis 18*, 2714−2723.
17. Gurevich, V. V., and Benovic, J. L. (2000) *Methods Enzymol. 315*, 422−437.
18. Schleicher, A., Kuhn, H., and Hofmann, K. P. (1989) *Biochemistry 28*, 1770−1775.
19. Gurevich, V. V. (1998) *J. Biol. Chem. 273*, 15501−15506.

BI992694Y